

Cite this: *J. Mater. Chem. C*, 2018, 6, 2303

Supramolecular self-assembly of thiol functionalized pentaalkynylbenzene-decorated gold nanoparticles exhibiting a room temperature discotic nematic liquid crystal phase†

Monika Gupta,^a Subhransu Sekhar Mohapatra,^b Surajit Dhara^b and Santanu Kumar Pal^{*a}

Thiol terminated pentaalkynylbenzene (PA) units were synthesized for coating on gold nanoparticles (GNPs) in order to obtain materials with a combination of the properties of GNPs and discotic nematogens. The PA unit with the longest terminal alkyl spacer was found to exhibit a discotic nematic (N_D) mesophase at room temperature which was preserved even after coating them on GNPs. The effect of GNPs on the orientational order parameter and the dielectric properties of the N_D mesophase have been investigated from various physical measurements. To the best of our knowledge, this is the first example of a room-temperature discotic nematic liquid crystal made of gold nanoparticles.

Received 28th November 2017,
Accepted 31st January 2018

DOI: 10.1039/c7tc05444k

rsc.li/materials-c

Introduction

While a limited number of discotic liquid crystals (DLCs) showing a nematic phase (N_D) have been reported in the literature, they are of great importance in many display device applications.¹ They have received particular interest since their commercialization as optical compensation films for enlarging the viewing angle of commonly used LC displays.² Unfortunately, most of the discotics possess N_D mesophases at high temperature and over a small temperature range.³ However, for application in devices, a N_D phase at room temperature is immensely essential.⁴

Furthermore, grafting LCs on a metal cluster such as gold nano-particles (GNPs) offers a combination of the properties of LCs with the size-dependent characteristics of GNPs. The inherent property of LCs to form mesophases due to their shape and polarizability anisotropy also influences the self-assembly of GNPs, whereas the GNPs affect the electro-optic and alignment properties of LCs in devices leading to collective advantages for both the components.⁵ However, achieving an LC phase in GNPs is quite a challenging task. Generally, to obtain a mesophase in such a system, the size of the GNPs should be sufficiently small so as to minimize the surface-anchoring effect of the LCs and thus they can behave the same as in the bulk phase.⁶

Furthermore, crowding of LC molecules at the surface of GNPs should also be avoided as that can lead to reduced mobility of the mesogens with a total loss of LC behaviour. For this purpose, a dendritic kind of molecules can be employed which will direct the LC molecules to position themselves at a distance from each other.⁷ Because of the design challenges imposed, most of the GNPs coated with LC molecules have been found to be non-LC.⁸ Several reports are available in the literature where these non-LC GNPs were dispersed in the LC materials.⁹ These LC-GNP composites have shown enhanced processability, plasma-emitting properties as well as interesting applications in opto-electronics, catalysis, electrically controlled light-scattering properties *etc.*¹⁰ These nano-composites have also shown a drastic enhancement in the dielectric behaviour resulting in their remarkably enhanced switching speeds as compared to the pure LCs.¹¹

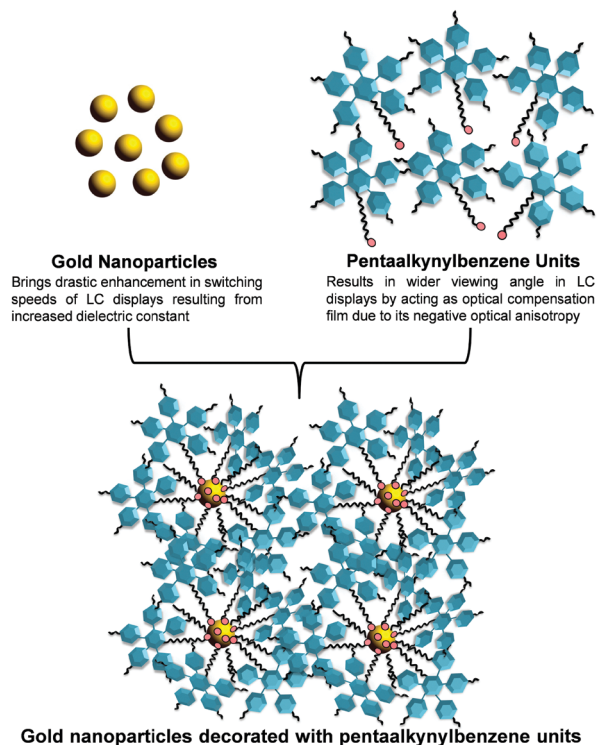
Investigation of a low-ordered nematic phase (where only orientational order is present) provides a promising approach if we take into account the design challenges imposed for a GNP-LC system. Moreover, for practical applications, a key challenge is to obtain GNPs in which the LC phase can be made stable at room temperature and over a wide temperature range. Till now, only three reports are available in the literature as reported by Mehl and co-workers which has described the synthesis of nematic LC GNPs.^{6,12} Among them, one of the LC gold nanoparticle systems exhibited a nematic mesophase at room temperature.^{12b} All these reports are based on laterally connected mesogens (calamitic) to the GNPs. This lateral connection not only provided a control over the size of GNPs but also prevented the crowding of mesogens at the gold surface leading to the

^a Department of Chemical Sciences, Indian Institute of Science Education and Research (IISER) Mohali, Sector-81, Knowledge City, Manauli-140306, India.

E-mail: skpal@iisermohali.ac.in, santanupal.20@gmail.com

^b School of Physics, University of Hyderabad, Hyderabad-500046, India

† Electronic supplementary information (ESI) available: Detailed synthetic procedure, characterization details, POM, DSC and SAXS/WAXS studies. See DOI: 10.1039/c7tc05444k



Scheme 1 Design of the gold nanoparticles decorated with pentaalkynylbenzene units synthesized in this study.

formation of a room-temperature mesophase. Surprisingly, till today, there are no reports on a N_D mesophase made of gold nanoparticles. In this paper, we have investigated the first LC GNP system that exhibits a room temperature N_D phase over a wide temperature range.

Here, we have synthesized GNPs decorated with thiol terminated pentaalkynylbenzene (PA) units (Scheme 1). The PA derivatives are known to form a N_D mesophase due to rotational freedom provided by the ethynyl linkers which avoids column formation.³ It has been observed in the earlier reports that GNPs coated with triphenylene, cyanobiphenyl *etc.* were found to be non-LC.¹³ In our approach, we have chosen the conformationally flexible PA units for coating GNPs whose size was regulated to be in the range of 2–3 nm. The PA units when attached to these smaller sized GNPs can induce a N_D LC phase by avoiding crowding on the surface of GNPs due to their dendritic structure. We hypothesized that when PA units are attached to smaller GNPs, the resulting system could be disordered enough to prevent efficient packing of the PA-GNPs and thus, may lead to the realization of a room temperature N_D phase. Furthermore, since PA units are optically negative birefringent ($\Delta n = n_e - n_o$, where n_e and n_o are the extraordinary and ordinary refractive indices, respectively), these LC GNPs are not only capable of showing improved opto-electronic properties but can also serve as compensation foils in the LC display devices.

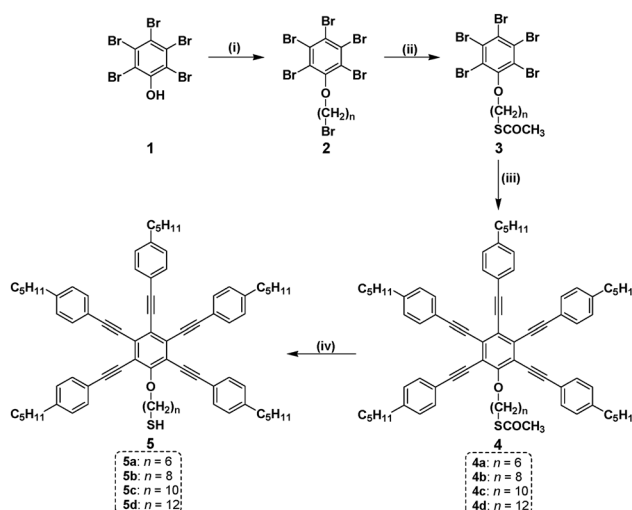
We first synthesized a series of thiol terminated PA derivatives. Interestingly, we found that one of the derivatives with the longest alkyl spacer displayed a N_D phase even at room temperature while the others stabilized a N_D phase at room temperature

upon cooling from the isotropic phase. The N_D phase has been well characterized by polarized optical microscopy (POM) and X-ray scattering studies (SAXS/WAXS). Furthermore, we have coated these thiol terminated derivatives on GNPs and found that coating with the longest alkyl spacer retained the N_D phase at room temperature. To study the effect of GNPs, we have also carried out temperature- and voltage-dependent dielectric and birefringence studies and compared it with pure thiol.

Results and discussion

Thiol terminated PA derivatives **5** were prepared using the synthetic route outlined in Scheme 2. Synthesis of compounds **2**, **3** and **4** was carried out following earlier reported procedures.¹⁴ For the synthesis of the final compound **5**, compound **4** was dissolved in a 1 : 1 mixture of dichloromethane and methanol. To that mixture, potassium carbonate was added and it was stirred for around 5 hours at room temperature to obtain the crude product which was further purified *via* column chromatography to yield the pure compound **5** (see the ESI† for details). All the synthesized compounds **5a–d** were characterized using ¹H NMR, ¹³C NMR, IR, UV-vis and mass spectrometry (ESI,† Fig. S1–S19).

The thermal behaviour of compounds **5** (precise transition temperatures and respective enthalpy changes) was examined using differential scanning calorimetry (DSC) and the mesophase behaviour was further explored *via* POM and SAXS/WAXS. Compound **5a** was solid at room temperature and displayed a crystal to N_D mesophase transition at 58.2 °C followed by isotropization at 110 °C (Table 1). On cooling, the mesophase appeared at 104 °C and remained stable up to –10.2 °C. Similarly, compounds **5b** and **5c** melted at around 59.8 °C and 66 °C to form the N_D mesophase (Fig. 1a), which clears at 68.9 °C and 83.8 °C, respectively. On cooling, the mesophase appeared at 41 °C and



Scheme 2 Synthesis of the target compounds **5**. Reagents and conditions: (i) K_2CO_3 , KI, $Br-(CH_2)_n-Br$, butanone, 80 °C, 18 h, 88%; (ii) $KSCoCH_3$, DMF, RT, 8 h, 80%; (iii) $Pd(PPh_3)_2Cl_2$, 4-pentylphenylacetylene, PPh_3 , CuI , Et_3N , 100 °C, 15 h, 85%; (iv) K_2CO_3 , $MeOH:CH_2Cl_2$ (1 : 1), 5 h, 50%.

Table 1 Thermal behaviour of the synthesized compounds **5**^{a,b}

Compound	Heating scan	Cooling scan
5a	Cr 58.2 (0.51) N_D 110 I	I 104 N_D -10.2 (4.72) Cr
5b	Cr 59.8 (4.34) N_D 68.9 (0.18) I	I 41 N_D -29.7 (1.38) Cr
5c	Cr 66 (4.0) N_D 83.8 (0.58) I	I 47 N_D -15.7 (1.70) Cr
5d	N_D 50 (0.49) I	I 43 N_D -27.2 (3.70) Cr

^a Phase transition temperatures (peak) in °C and transition enthalpies in kJ mol^{-1} (in parentheses). ^b Phase assignments: Cr = Crystalline, N_D = discotic nematic, I = isotropic. Some of the transitions were not observed in the DSC scan, however, they were confirmed from POM studies.

47 °C which transformed to the crystalline state at -29.7 °C and -15.7 °C for **5b** and **5c**, respectively. Interestingly, compound **5d** existed in the LC state even at room temperature and became isotropic at 50 °C on heating the sample.

On cooling back from the isotropic state, a Schlieren texture (typical of N_D phase) appeared at 43 °C which further crystallized at -27.2 °C (Fig. 1b and ESI,† Fig. S20, S21). The compounds of series **4** also exhibited mesomorphic behaviour. Additionally, two of the compounds **4c** and **4d** displayed N_D phase even at room temperature on cooling from the isotropic phase (ESI,† Table S1 and Fig. S22, S23).

The quantitative study of the nematic phases of all the compounds of series **5** was investigated *via* SAXS/WAXS studies (Fig. 1c). All the compounds of series **5** in their mesophase displayed one narrow reflection in the small angle region and one broad peak in the wide angle regime, respectively. This pattern confirms the presence of a N_D phase. The compounds of series **4** also displayed similar diffractograms to those of

series **5** in their mesophase (ESI,† Fig. S24 and Table S2). For compound **5a**, the calculated d -spacing of around 19.95 Å for the signal in the small angle region corresponds to the separation between the PA units and thus approximates the diameter of a single PA disc (~19 Å). The spacing of the wide angle peak is 4.93 Å which originates from the liquid-like correlation of the molten chains. The diffraction patterns corresponding to the nematic phases of compounds **5b**, **5c** and **5d** are very identical to **5a** and analysed in a similar way.

The correlation length, *i.e.*, the degree of order within the mesophase, was calculated from the Scherrer's equation.¹⁵ For compound **5a**, the correlation lengths for the reflections at 19.95 Å and 4.93 Å are calculated to be 39.18 Å and 9.22 Å, respectively. In order to measure spatial order in terms of the molecular length scale, the correlation length was divided by the d -spacing values (Table 2). The respective correlation lengths for compounds **5** were found to decrease with increasing chain length of the alkyl spacer.

The decrease in correlation length is significant for the reflection corresponding to the small-angle region (Table 2). This can be due to the fact that compounds **5** are discotic mesogens based on pentakis(phenylethynyl)benzene composed of flexible alkyl chains and a terminal thiol group (Fig. 1d). In the case of PA, the phenyl rings are generally not in plane because of rotational freedom provided by ethynyl linkers which prevents columnar stacking. Furthermore, orientational freedom of the PA group increases on increasing the terminal alkyl chain length which is also reflected in the decreasing value of the corresponding correlation lengths.

Our next goal was to synthesize and characterize GNPs coated with PA units. The preparation of GNPs was carried out by closely

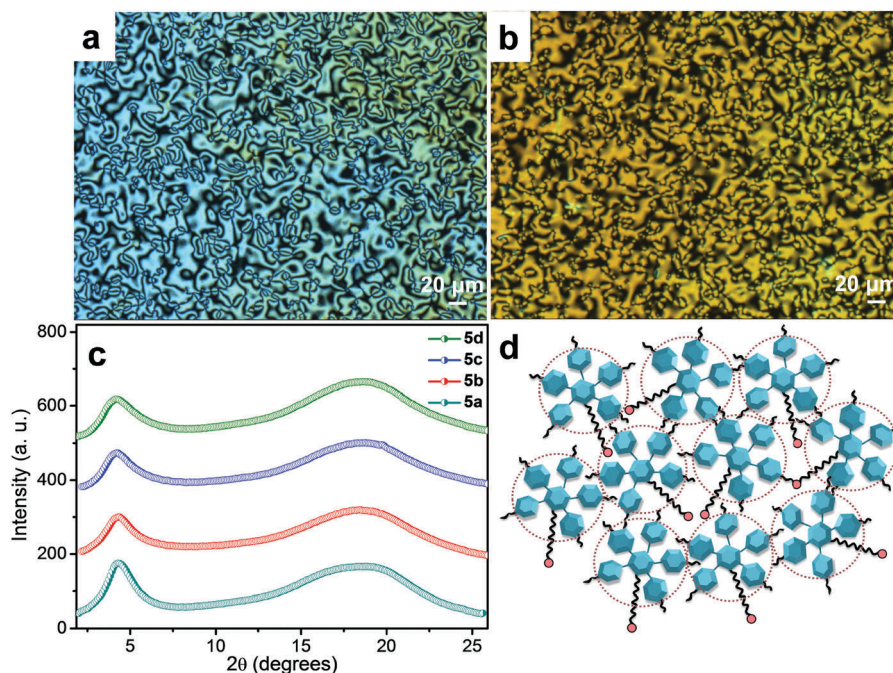


Fig. 1 Optical photomicrograph of compound (a) **5c** at 36.6 °C and (b) **5d** at 41.8 °C representing the N_D phase (on cooling from isotropic, crossed polarizers). (c) X-ray diffraction pattern of compounds **5a–d** in the nematic phase. (d) The schematic representation of the arrangement of PA units in the mesophase.

Table 2 X-ray reflections and corresponding correlation lengths in the discotic nematic phases of compound **5a–d**

Compound	Properties	Small angle peak	Wide angle peak
5a	<i>d</i> -Spacing (Å)	19.95	4.93
	Correlation length (ξ) (Å)	39.18	9.22
	ξ/d	1.96	1.87
5b	<i>d</i> -Spacing (Å)	19.96	4.89
	Correlation length (ξ) (Å)	36.60	10.58
	ξ/d	1.83	2.16
5c	<i>d</i> -Spacing (Å)	19.9	4.87
	Correlation length (ξ) (Å)	34.97	9.78
	ξ/d	1.75	2.00
5d	<i>d</i> -Spacing (Å)	19.99	4.85
	Correlation length (ξ) (Å)	30.81	9.17
	ξ/d	1.54	1.89

following an earlier reported method (see the Experimental section for details).¹⁶ All the synthesized GNPs were characterised using ¹H NMR, UV-vis and TEM analysis. Their thermotropic behaviour was analysed *via* POM, DSC and further characterized using SAXS/WAXS techniques. The ¹H NMR spectra of the synthesized nanoparticles displayed broadened peaks as compared to those obtained for thiols and thus indicates that thiols are attached to the surface of gold nanoparticles and are not present in their free form (ESI,† Fig. S25). Furthermore, a characteristic peak at 517 nm in the UV-vis spectra arises due to surface plasmon resonance and represents the formation of spherical GNPs (ESI,† Fig. S26).¹⁷

We have found that GNPs with shorter chain lengths *i.e.* **5a–c** GNPs were sticky solids at room temperature and displayed

an increase in birefringence with some phase separation occurring on heating. On cooling, they did not display any birefringence till room temperature and existed as isotropic liquids during the second heating/cooling cycles. A possible reason for this behaviour could be because of the non-uniform coverage of the capping agent on the gold cluster due to steric hindrance arising from the shorter chain length of the terminal alkyl chain. Interestingly, in contrast to the above observations, **5d**-GNPs were very stable and displayed an enantiotropic mesophase which existed even at room temperature. Therefore, we have discussed **5d**-GNPs in detail in the next section.

The **5d**-GNPs were displaying birefringence with shearability of textures at room temperature which confirms the presence of a LC phase which on heating converted to isotropic liquid at 60 °C (Fig. 2a). On further cooling, a Schlieren texture typical of a nematic mesophase was observed at 57 °C which remained stable up to –12.95 °C (Fig. 2b and ESI,† Fig. S27). It can be thus inferred that the room temperature *N_D* phase of **5d** was retained even after coating **5d** on the GNPs. However, the mesophase range was shifted to a higher temperature as compared to pure thiol **5d**.

The size of the **5d**-GNPs was found to be in the range of 2.5–3.1 nm from TEM observations (Fig. 2c). Dynamic light scattering measurements also indicated the formation of GNPs with a size of ~2.76 nm with a polydispersity index of 0.35. The number of mesogens attached to a single GNP was found to be around 263 from TGA analysis (ESI,† Fig. S28). The mean formula for **5d**-GNPs is found to be Au₅₇₄(PA)₂₆₃. The nematic mesophase exhibited by **5d**-GNPs was further characterised *via* SAXS/WAXS studies (Fig. 2d and e).

The XRD pattern exhibited two peaks: one sharp peak at a small-angle and another diffuse peak in the wide-angle

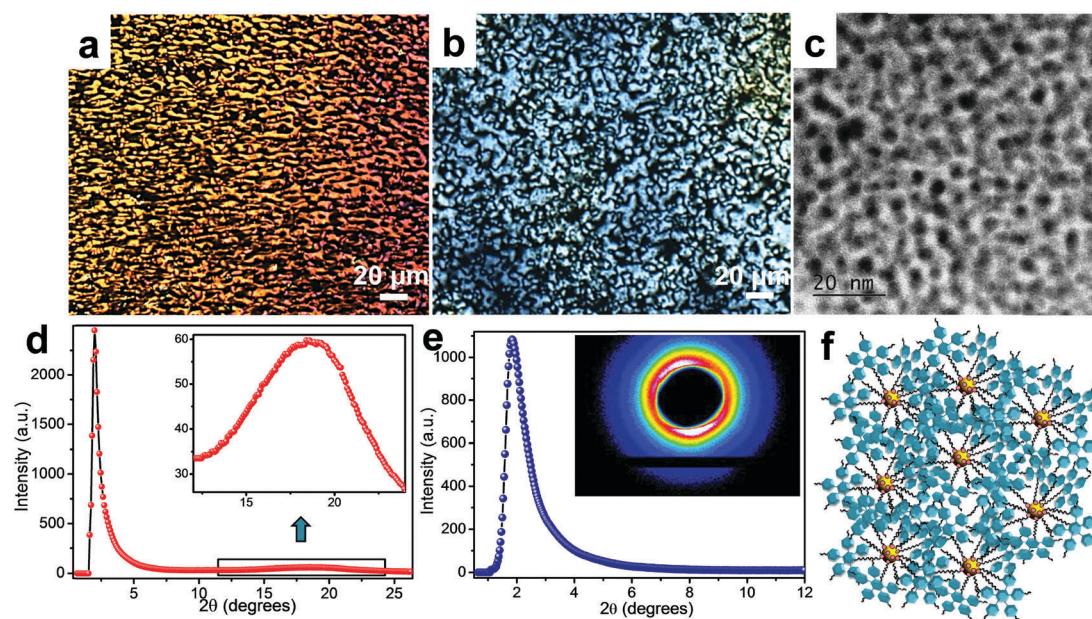


Fig. 2 The POM textures of **5d**-GNPs (a) on heating at 45 °C and (b) on cooling from the isotropic at 40 °C (crossed polarizers, magnification: $\times 200$). (c) TEM image of **5d**-GNPs obtained by dispersing the dilute solution of **5d**-GNPs in toluene on a carbon coated copper grid. (d) The wide-angle X-ray scattering (WAXS), (e) small-angle X-ray scattering (SAXS) pattern of **5d**-GNPs in the *N_D* phase at room-temperature and (f) their schematic representation in the *N_D* mesophase.

region (Fig. 2d). In our case, the nematic gold nanoparticles are possibly intercalated and the observed d -spacing (42.68 Å) in the small angle, likely corresponds to the average side by side separation between centres of two GNPs covered with PA units. The peak in the wide angle regime observed at 4.86 Å corresponds to liquid like correlation of the molten alkyl chains. Fig. 2e shows the **5d**-GNP modelled as a gold cluster surrounded by PA units and the arrangement of the model units in the nematic mesophase. The correlation lengths for the reflections at 42.68 Å and 4.86 Å are calculated to be 135.16 Å and 14.72 Å, respectively. For measuring the spatial order in terms of the molecular length scale, the correlation length was divided by the d -spacing values which were around 3.16 Å and 3.02 Å for the peak at a small- and wide-angle, respectively, and is about double of the values as observed for compound **5d**. A reason for the stabilization of the mesophase in the case of the **5d**-GNPs could be due to a longer terminal alkyl spacer length of thiol **5d** which avoids crowding of the mesogens on the gold surface and thus ensures a uniform coating of mesogens on the GNPs which may not be feasible in the case of shorter spacer length of thiols **5a–c**. We have excluded the layering or other packing from the POM as well as XRD studies. In POM, we can easily observe the Schlieren texture which is typical of a nematic mesophase. Furthermore, in the XRD studies we did not observe any higher order peak which excludes the possibility of any positional order among the mesogens.

It should be noted that TEM studies only indicate the size of gold core which we found to be in the range of 2.5–3.1 nm. The TEM studies were carried out by drop casting a very dilute **5d**-GNP solution in toluene onto a carbon supported copper grid (200 Mesh Cu). However, the distance between two gold nanoparticles was found to be about ~ 3.3 nm which is less

than the ligand diameter indicating partial intercalation of PA units. A DLS study was also performed in a dilute **5d**-GNP solution in toluene. The obtained particle sizes (~ 2.76 nm) was in very close agreement with the TEM results. The XRD was carried out in Lindeman capillary in the nematic phase itself. It gives an average length of the GNPs covered with the PA mesogens, which is expected to be higher than the size of only the gold core.

To investigate the physical properties and bring out the effect of the GNPs, we have conducted birefringence and dielectric measurements. The details of the experimental techniques have been reported previously.¹⁸ We used polyimide (AL-1254) coated cells with antiparallel rubbing. Such cells provide planar alignment of the calamitic nematic LCs. In the case of N_D LCs, it provides homeotropic alignment of the director (*i.e.* the plane of discs is parallel to the substrates). Fig. 3a shows the voltage dependent effective dielectric constant (ϵ_{eff}) for compounds **5d** and **5d**-GNPs. ϵ_{eff} is slightly larger for the **5d**-GNPs as compared to **5d**. It shows a small increase beyond a particular voltage and gets saturated at a much higher voltage. At the low voltage, the director is perpendicular to the substrate and at the higher voltage (above the Fréedericksz threshold voltage, V_{th}) it turns parallel.

The increase of ϵ_{eff} with voltage in both the samples indicates that they have a negative dielectric anisotropy and their values are very small ($\Delta\epsilon \approx -0.1$). Fig. 3b shows the variation of ϵ_{eff} (*i.e.*, ϵ_{II}) in the nematic phase measured at a fixed voltage of 18 V. It shows that ϵ_{II} is almost constant in the nematic phase and it is higher by about 10% in the **5d**-GNPs than in **5d**. Fig. 3c shows the variation of birefringence (Δn) with applied voltage. We observed that beyond the Fréedericksz threshold voltage ($V_{\text{th}} \cong 2$ V), Δn increases and saturates beyond 15 V. This means

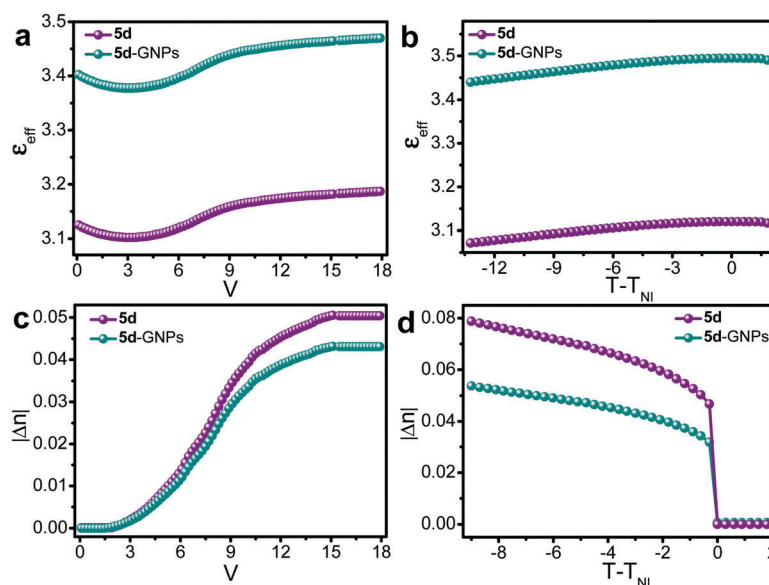


Fig. 3 (a) Voltage-dependent dielectric constant of compound **5d** at a fixed temperature $T - T_{\text{NI}} = -3.59$ °C and **5d**-GNPs at a fixed temperature $T - T_{\text{NI}} = -4.0$ °C. (b) Temperature-dependent dielectric constant of compound **5d** and **5d**-GNPs at a fixed voltage of 18 V and a frequency of 2 kHz. (c) Voltage-dependent birefringence (Δn) of **5d** at a fixed temperature of $T - T_{\text{NI}} = -3.78$ °C and of **5d**-GNPs at a fixed temperature of $T - T_{\text{NI}} = -6.20$ °C. (d) Temperature-dependent birefringence (Δn) of **5d** and **5d**-GNPs at a fixed voltage of 20 V and frequency of 2 kHz.

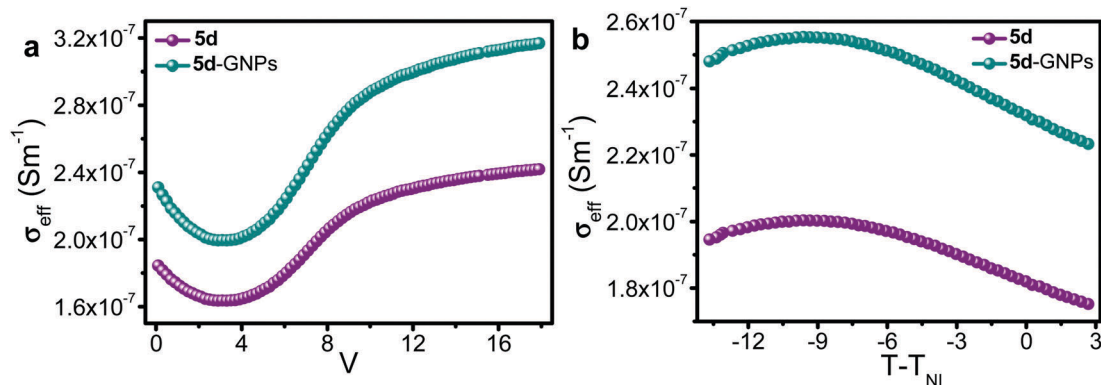


Fig. 4 (a) Variance of conductivity of **5d** and **5d**-GNPs at a fixed temperature (-2.50 $^{\circ}\text{C}$). (b) Temperature variation of conductivity of **5d** and **5d**-GNPs at a fixed voltage of 18 V and a frequency of 2 kHz.

that the director of the N_{D} mesogens is completely re-orientated to the planar state. Fig. 3d shows the temperature dependent variation of the birefringence measured at a fixed voltage of 18 V. It is observed that Δn in the compound **5d**-GNPs is significantly shorter than in compound **5d**. For example, at $T - T_{\text{NI}} = -9$ $^{\circ}\text{C}$, Δn in **5d**-GNPs is about 40% smaller than that of **5d**.

Since Δn is proportional to the orientational order parameter S , we conclude that the inclusion of gold nanoparticles has reduced the order parameter significantly and this is consistent with our proposed model presented in Fig. 2f where the GNPs are surrounded by PA units.

We further measured the effective electrical conductivity (σ_{eff}) of the sample as a function of voltage and temperature. The frequency of measurements is 2 kHz and only ionic conductivity is expected to contribute in the measurements. Fig. 4a shows that **5d**-GNPs has a larger conductivity than that of **5d**. With increasing voltage, σ_{eff} slightly decreases below the Fréedericksz threshold voltage, $V_{\text{th}} = 2$ V, followed by an increase at a higher voltage. The decrease of σ_{eff} below V_{th} could be due to the reduction of the bulk charge density due to selective ion absorptions at the electrodes. Since the conductivity along the director is expected to be larger than in the perpendicular direction, the increase in σ_{eff} at a higher voltage in both the compounds cannot be due to reorientation of the director. This could be attributed to an increase in the mobility of the charges at a higher voltage. Fig. 4b shows the temperature dependent variation of σ_{II} for both the compounds measured at a frequency of 2 kHz. σ_{II} in **5d**-GNPs is about 30% larger than that of **5d**. Therefore, it can be inferred that incorporation of GNPs has reduced the orientational order parameter and enhanced the electrical conductivity significantly. The enhancement in the dielectric and conductivity in **5d**-GNPs are expected due to the Maxwell-Wagner effects.¹⁹

Conclusions

In summary, this report describes for the first time the synthesis of GNPs decorated with thiol functionalized PA units which exhibits a N_{D} phase at room temperature. These N_{D} GNPs have shown an enhanced dielectric response and increased conductivity

values as compared to the thiols. Therefore, these GNPs exhibiting a N_{D} mesophase at room temperature are very interesting materials for display applications and also points the way towards the development of new anisotropic soft materials for their usability in devices.

Experimental section

Preparation of thiol-coated gold nanoparticles

For the preparation of thiol-coated GNPs, a solution of tetraoctylammonium bromide (0.124 mmol) in toluene (5 ml) was prepared and added to an aqueous solution of $\text{HAuCl}_4 \cdot 3\text{H}_2\text{O}$ (0.028 mmol). The resulting solution was stirred for 20 minutes to ensure a complete transfer of gold chloride from the aqueous to organic layer. The organic layer was separated and washed with distilled water. A solution of thiol (0.038 mmol) in toluene (2 ml) was added to the above solution and the resulting mixture was stirred for 30 minutes. An aqueous solution of NaBH_4 (0.28 mmol) was added dropwise to the above solution and the mixture was stirred for a further period of 6 h. The toluene layer was washed with distilled water, diluted with methanol (250 ml) and kept in a refrigerator overnight. The precipitate obtained was purified by re-suspending in toluene and was then centrifuged after the addition of methanol (10 ml). This purification step was repeated several times to ensure the complete removal of any non-covalently bound organic material. Full characterization details, TGA, DSC, POM textures are provided in the ESI.†

Characterization

Structural characterization of the compound was carried out through a combination of infrared spectroscopy (Perkin Elmer Spectrum AX3), ^1H NMR and ^{13}C NMR (Bruker Biospin Switzerland Avance-iii 400 MHz and 100 MHz spectrometers respectively), UV-vis-NIR spectrophotometer (Agilent Technologies UV-vis-NIR Spectrophotometer) and mass spectrometry (Waters synapt G2s). NMR spectra were recorded using deuterated chloroform (CDCl_3) as the solvent and tetramethylsilane (TMS) as an internal standard. DSC measurements were performed using a Perkin Elmer DSC 8000 coupled to a Controlled Liquid Nitrogen Accessory (CLN 2) with a scan rate of 5 $^{\circ}\text{C min}^{-1}$. Textural observations of the

mesophase were performed using a Nikon Eclipse LV100POL polarising microscope provided with a Linkam heating stage (LTS 420). All images were captured using a Q-imaging camera. X-ray diffraction (XRD) was carried out on powder samples using Cu K α ($\lambda = 1.54 \text{ \AA}$) radiation from a source (GeniX 3D, Xenocs) operating at 50 kV and 0.6 mA. The diffraction patterns were collected on a two module Pilatus detector.

Materials

Chemicals and solvents were all of AR quality and were used without further purification. Pentabromophenol, 1-ethynyl-4-pentylbenzene, copper iodide, bis(triphenylphosphine) palladium(II) dichloride, triphenylphosphine, triethylamine, dibromohexane, dibromooctane, dibromodecane, dibromododecane, potassium carbonate, potassium iodide, potassium thioacetate, methanol, butanone, dimethylformamide and dichloromethane were all purchased from Sigma-Aldrich (Bangalore, India). Column chromatographic separations were performed on silica gel (60–120, 100–200 & 230–400 mesh). Thin layer chromatography (TLC) was performed on aluminium sheets pre-coated with silica gel (Merck, Kieselgel 60, F254).

Conflicts of interest

There are no conflicts to declare.

Acknowledgements

We are grateful to the NMR, HRMS and SAXS/WAXS facility at IISER Mohali. Dr SK Pal and Dr S Dhara are grateful for financial support from INSA (bearing sanction No. SP/YSP/124/2015/433) and DST, FIST-II (University of Hyderabad), respectively. SKP acknowledges CSIR Project File No. 02(0311)/17/EMR-II. M. Gupta acknowledges the receipt of a graduate fellowship from IISER Mohali.

Notes and references

- (a) S. Kumar, *Chem. Soc. Rev.*, 2006, **35**, 83–109; (b) T. Wöhrle, I. Wurzbach, J. Kirres, A. Kostidou, N. Kapernaum, J. Litterscheidt, J. C. Haenle, P. Staffeld, A. Baro, F. Giesselmann and S. Laschat, *Chem. Rev.*, 2016, **116**, 1139–1241; (c) S. Kumar, *Chemistry Of Discotic Liquid Crystals: From Monomers to Polymers*, CRS Press, Taylor & Francis Group, Boca Raton, 2011.
- (a) M. Lu and K. H. Yang, *Jpn. J. Appl. Phys.*, 2000, **39**, L412–L415; (b) H. Mori, Y. Itoh, Y. Nishuira, T. Nakamura and Y. Shinagawa, *Jpn. J. Appl. Phys.*, 1997, **36**, 143–147.
- H. K. Bisoyi and S. Kumar, *Chem. Soc. Rev.*, 2010, **39**, 264–285.
- (a) S. Kumar and S. K. Varshney, *Angew. Chem., Int. Ed.*, 2000, **112**, 3270–3272; (b) S. Kumar, S. K. Varshney and D. Chauhan, *Mol. Cryst. Liq. Cryst.*, 2003, **396**, 241–250; (c) S. K. Varshney, V. Prasad and H. Takezoe, *Liq. Cryst.*, 2011, **38**, 53–60; (d) S. Kohmoto, E. Mori and K. Kishikawa, *J. Am. Chem. Soc.*, 2007, **129**, 13364–13365; (e) S. C. Chien, H. H. Chen, H. C. Chen, Y. L. Yang, H. F. Hsu, T. L. Shih and J. J. Lee, *Adv. Funct. Mater.*, 2007, **17**, 1896–1902; (f) H.-H. Chen, H.-A. Lin, S.-C. Chien, T.-H. Wang, H.-F. Hsu, T.-L. Shih and C. Wu, *J. Mater. Chem.*, 2012, **22**, 12718–12722; (g) M. Gupta, S. P. Gupta, M. V. Rasna, D. Adhikari, S. Dhara and S. K. Pal, *Chem. Commun.*, 2017, **53**, 3014–3017; (h) M. Gupta, S. P. Gupta, S. S. Mohapatra, S. Dhara and S. K. Pal, *Chem. – Eur. J.*, 2017, **23**, 10626–10631.
- (a) S. Kumar, *NPG Asia Mater.*, 2014, **6**, 1–13; (b) H. K. Bisoyi and S. Kumar, *Chem. Soc. Rev.*, 2011, **40**, 306–319; (c) S. Kumar, *Liq. Cryst.*, 2013, **41**, 353–367; (d) S. Kumar and V. Lakshminarayanan, *Chem. Commun.*, 2004, 1600–1601; (e) T. Hegmann, H. Qi and V. M. Marx, *J. Inorg. Organomet. Polym. Mater.*, 2007, **17**, 483–508; (f) S. K. Prasad, K. L. Sandhya, G. G. Nair, U. S. Hiremath, C. V. Yelamaggad and S. Sampath, *Liq. Cryst.*, 2006, **33**, 1121–1125; (g) H. Qi, B. Kinkead and T. Hegmann, *Adv. Funct. Mater.*, 2008, **18**, 212–221; (h) H. Qi and T. Hegmann, *J. Mater. Chem.*, 2008, **18**, 3288–3294.
- L. Cseh and G. H. Mehl, *J. Mater. Chem.*, 2007, **17**, 311–315.
- (a) R. M. Richardson, S. A. Ponomarenko, N. I. Boiko and V. P. Shibaev, *Liq. Cryst.*, 1999, **26**, 101–108; (b) T. Kato, N. Mizohita and K. Kishimoto, *Angew. Chem., Int. Ed.*, 2006, **45**, 38–68.
- H. Qi and T. Hegmann, *Liq. Cryst. Today*, 2011, **20**, 102–114.
- A. Choudhary, G. Singh and A. M. Biradar, *Nanoscale*, 2014, **6**, 7743–7756.
- (a) L. Cseh and G. H. Mehl, *J. Am. Chem. Soc.*, 2006, **128**, 13376–13377; (b) X. B. Zeng, F. Liu, A. G. Fowler, G. Ungar, L. Cseh, G. H. Mehl and J. E. Macdonald, *Adv. Mater.*, 2009, **21**, 1746–1750; (c) H. Qi and T. Hegmann, *J. Mater. Chem.*, 2006, **16**, 4197–4205; (d) V. M. Marx, H. Girgis, P. A. Heiney and T. Hegmann, *J. Mater. Chem.*, 2008, **18**, 2983–2994; (e) A. N. Gowda, M. Kumar, A. R. Thomas, R. Phillip and S. Kumar, *ChemistrySelect*, 2016, **1**, 1361–1370; (f) M. Mishra, S. Kumar and R. Dhar, *RSC Adv.*, 2014, **4**, 62404–62412; (g) S. Kumar, S. K. Pal and V. Lakshminarayanan, *Mol. Cryst. Liq. Cryst.*, 2005, **434**, 251–258.
- (a) I. In, Y. W. Jim, Y. J. Kim and S. Y. Kim, *Chem. Commun.*, 2005, 800–801; (b) H. Qi and T. Hegmann, *J. Mater. Chem.*, 2006, **16**, 4197–4205; (c) H. Qi and T. Hegmann, *J. Mater. Chem.*, 2008, **18**, 3288–3294.
- (a) L. Cseh and G. H. Mehl, *J. Am. Chem. Soc.*, 2006, **128**, 13376–13377; (b) C. H. Yu, C. P. J. Schubert, C. Welch, B. J. Tang, M. G. Tamba and G. H. Mehl, *J. Am. Chem. Soc.*, 2012, **134**, 5076–5079.
- (a) H. Qi, B. Kinkead, V. M. Marx, H. R. Zhang and T. Hegmann, *Chem. Phys. Chem.*, 2009, **10**, 1211–1218; (b) S. Kumar, S. K. Pal, P. S. Kumar and V. Lakshminarayanan, *Soft Matter*, 2007, **3**, 896–900.
- (a) M. Gupta and S. K. Pal, *Liq. Cryst.*, 2015, **42**, 1250–1256; (b) M. Gupta, I. Bala and S. K. Pal, *Tetrahedron Lett.*, 2014, **55**, 5836–5840; (c) M. Gupta and S. K. Pal, *Langmuir*, 2016, **32**, 1120–1126; (d) M. Gupta, S. P. Gupta and S. K. Pal, *J. Phys. Chem. B*, 2017, **121**, 8593–8602; (e) S. Kumar and S. K. Pal, *Liq. Cryst.*, 2005, **32**, 659–661.

- 15 S. P. Gupta, M. Gupta and S. K. Pal, *ChemistrySelect*, 2017, **2**, 6070–6077.
- 16 B. I. Ipe, K. Yoosaf and K. G. Thomas, *J. Am. Chem. Soc.*, 2006, **128**, 1907–1913.
- 17 V. Amendola and M. Meneghetti, *J. Phys. Chem. C*, 2009, **113**, 4277–4285.
- 18 (a) S. Dhara and N. V. Madhusudana, *Europhys. Lett.*, 2004, **67**, 411–417; (b) P. Sathyanarayana, M. Mathews, Q. Li, V. S. S. Sastry, K. V. Le, H. Takezoe and S. Dhara, *Phys. Rev. E: Stat., Nonlinear, Soft Matter Phys.*, 2010, **81**, 010702(R); (c) P. Sathyanarayana, B. K. Sadashiva and S. Dhara, *Soft Matter*, 2011, **7**, 8556–8560; (d) P. Sathyanarayana, M. C. Varia, A. K. Prajapati, B. Kundu, V. S. S. Sastry and S. Dhara, *Phys. Rev. E: Stat., Nonlinear, Soft Matter Phys.*, 2010, **82**, 050701(R).
- 19 (a) J. C. Maxwell, *Treatise on Electricity and Magnetism*, Dover, New York, 1945, vol. 1, pp. 451–461; (b) S. Kobayashi, T. Miyama, N. Nishida, Y. Sakai, H. Shiraki, Y. Shiraishi and N. Toshima, *J. Disp. Technol.*, 2006, **2**, 121–129.